



Approaches to Study Gap Junctional Coupling

Jonathan Stephan^{1*}, Sara Eitelmann¹ and Min Zhou^{2*}

¹ Institute of Neurobiology, Heinrich Heine University Düsseldorf, Düsseldorf, Germany, ² Department of Neuroscience, Wexner Medical Center, Ohio State University, Columbus, OH, United States

OPEN ACCESS

Edited by:

Christian Lohr,
University of Hamburg, Germany

Reviewed by:

Gerald Seifert,
University Hospital Bonn, Germany
Luc Leybaert,
Ghent University, Belgium

*Correspondence:

Jonathan Stephan
jonathan.stephan@uni-duesseldorf.de
Min Zhou
Zhou.787@osu.edu

Specialty section:

This article was submitted to
Non-Neuronal Cells,
a section of the journal
Frontiers in Cellular Neuroscience

Received: 11 December 2020

Accepted: 03 February 2021

Published: 10 March 2021

Citation:

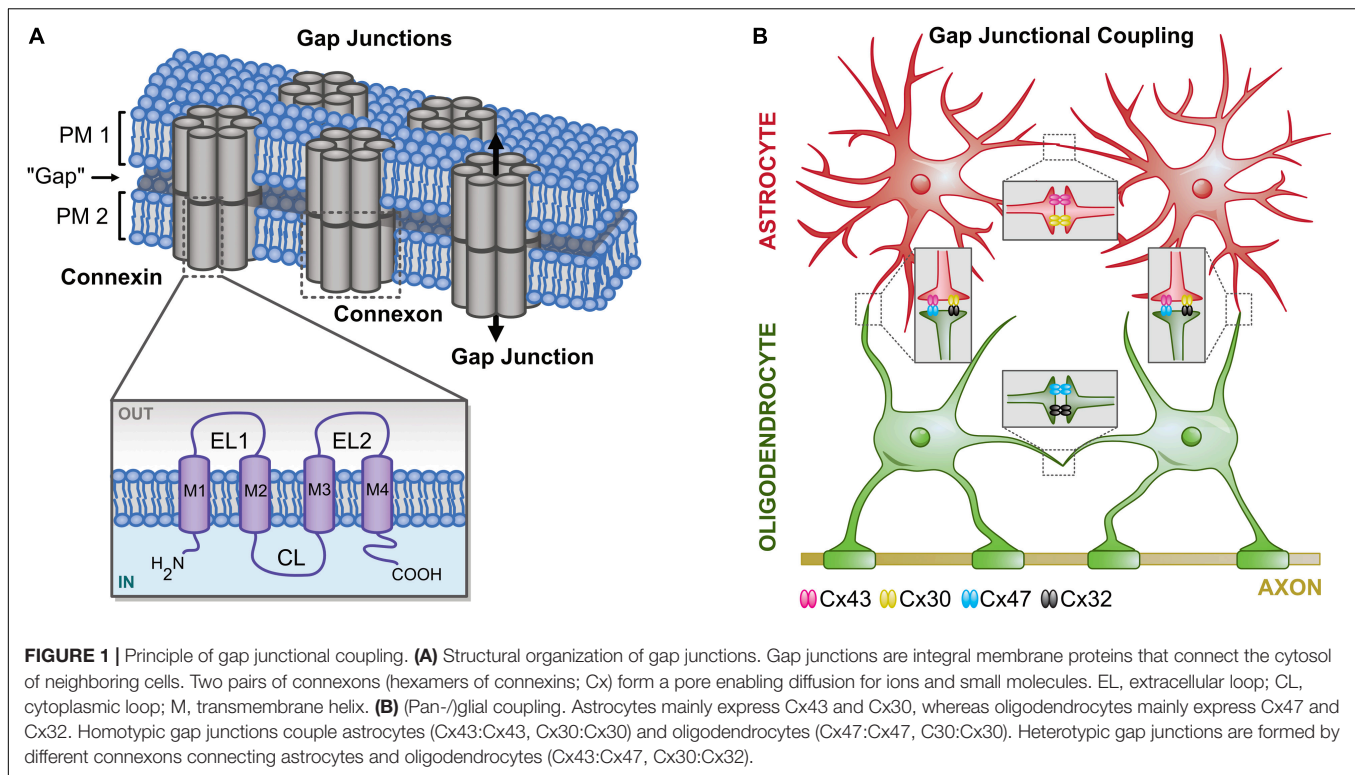
Stephan J, Eitelmann S and
Zhou M (2021) Approaches to Study
Gap Junctional Coupling.
Front. Cell. Neurosci. 15:640406.
doi: 10.3389/fncel.2021.640406

Astrocytes and oligodendrocytes are main players in the brain to ensure ion and neurotransmitter homeostasis, metabolic supply, and fast action potential propagation in axons. These functions are fostered by the formation of large syncytia in which mainly astrocytes and oligodendrocytes are directly coupled. Panglial networks constitute on connexin-based gap junctions in the membranes of neighboring cells that allow the passage of ions, metabolites, and currents. However, these networks are not uniform but exhibit a brain region-dependent heterogeneous connectivity influencing electrical communication and intercellular ion spread. Here, we describe different approaches to analyze gap junctional communication in acute tissue slices that can be implemented easily in most electrophysiology and imaging laboratories. These approaches include paired recordings, determination of syncytial isopotentiality, tracer coupling followed by analysis of network topography, and wide field imaging of ion sensitive dyes. These approaches are capable to reveal cellular heterogeneity causing electrical isolation of functional circuits, reduced ion-transfer between different cell types, and anisotropy of tracer coupling. With a selective or combinatory use of these methods, the results will shed light on cellular properties of glial cells and their contribution to neuronal function.

Keywords: patch clamp, paired recordings, astrocyte syncytial isopotentiality, tracer coupling, wide field imaging

INTRODUCTION

Gap junction channels connect the cytosol of neighboring cells and allow the exchange of ions and small molecules, such as metabolites (Giaume et al., 2010, 2020). Gap junctions form, when two connexons in the membrane of neighboring cells align. Connexons in turn are hexamers that are formed by connexins (Cx; **Figure 1A**). There are 21 Cxs identified so far of which 11 are expressed by neurons and glial cells in the CNS that differ in their mass (Bedner et al., 2012) and expression profile (including developmental and cell type specificity) (Dahl et al., 1996; Kunzelmann et al., 1999; Nagy et al., 1999; Nagy and Rash, 2000; Augustin et al., 2016; Wadle et al., 2018). The composition of gap junctions with different connexons and Cxs defines their properties, for example selectivity and permeability (Bukauskas and Verselis, 2004; Harris, 2007; Abbaci et al., 2008). In addition, post-translational modifications further regulate gap junctional communication (Goodenough and Paul, 2009; Axelsen et al., 2013; Aasen et al., 2018). Homocellular coupling between astrocytes and oligodendrocytes is mediated by homotypic gap junctions (**Figure 1B**; Giaume and Theis, 2010; Maglione et al., 2010). Furthermore, heterocellular (panglial) coupling is observed between both cell types using heterotypic gap junctions (Wasseff and Scherer, 2011; Griemsmann et al., 2015; Augustin et al., 2016; Moshrefi-Ravasdjani et al., 2017; Claus et al., 2018; Wadle et al., 2018; Xin et al., 2019).



In the corpus callosum, astrocytes and NG2 glia form panglial networks (Moshrefi-Ravasdjani et al., 2017). However, in many other brain regions—like the hippocampus, the cortex, and the medial nucleus of the trapezoid body—NG2 glia are neither tracer nor electrically coupled to other glial cells (Wallraff et al., 2004; Houades et al., 2008; Muller et al., 2009; Xu et al., 2014; Bedner et al., 2015; Griemsmann et al., 2015).

Gap junctional coupling is important for homeostasis of K^+ (Wallraff et al., 2006; Pannasch et al., 2011; Breithausen et al., 2020; MacAulay, 2020), Na^+ (Langer et al., 2012; Augustin et al., 2016; Moshrefi-Ravasdjani et al., 2017; Wadle et al., 2018), Cl^- (Egawa et al., 2013), and neurotransmitters (Pannasch et al., 2011; Chaturvedi et al., 2014). Furthermore, regulated gap junctional coupling is mandatory for activity-dependent redistribution of metabolites, such as glucose (Cruz et al., 2007; Rouach et al., 2008; Giaume et al., 2010). In addition, Cx expression and gap junctional communication are altered under pathophysiological conditions (Cotrina et al., 1998; Nakase et al., 2006; Giaume et al., 2010, 2019, 2020; Xu et al., 2010; Bedner et al., 2015; Lee et al., 2016; Wang Q. et al., 2020). Thus, the basic knowledge about glial gap junctional communication is fundamentally important for our further understanding of the complex neuron-glia interaction in healthy and diseased brains.

Astrocytes can be identified by several approaches. Many astrocytes express marker proteins such as GFAP, S100 β , GLAST, or GLT-1 (Eng et al., 2000; Zhou et al., 2006; Kafitz et al., 2008; Schreiner et al., 2014). However, there are subpopulations of astrocytes, which for example do not express GFAP (Kafitz et al., 2008). Additionally, a fraction of NG2 glia are characterized by expression of GFAP and S100 β

(Nolte et al., 2001; Matthias et al., 2003; Karram et al., 2008). In 2004, the red fluorescent dye sulforhodamine (SR) 101 was introduced as a marker for astrocytes (Nimmerjahn et al., 2004), which allows the *a priori* identification of classical astrocytes in various brain regions, for example, in hippocampus, cortex, and auditory brainstem (Nimmerjahn et al., 2004; Kafitz et al., 2008; Stephan and Friauf, 2014; Ghirardini et al., 2018). Additionally, the use of SR101 is particularly advantageous in astrocyte imaging experiments as it can be combined with ion sensitive dyes such as Fura-2 and sodium-binding benzofuran isophthalate (SBFI; Kafitz et al., 2008; Langer et al., 2012).

Another approach for *a priori* identification of astrocytes is the utilization of reporter mice, such as GFAP-eGFP mice (Nolte et al., 2001). However, the transcript labels only a subset of astrocytes (Nimmerjahn et al., 2004) and, moreover, the transcript is also weakly expressed by NG2 glia (Matthias et al., 2003). Alternatively, ALDH1L1-eGFP mice can be used to identify astrocytes (Heintz, 2004; Yang et al., 2011). These reporter mice exhibit a more accurate labeling pattern of astrocyte populations (Cahoy et al., 2008). Aside this, reporter mice are available to *a priori* identify other glia, such as oligodendrocytes (PLP-GFP mice; Fuss et al., 2000) or NG2 glia (NG2-eYFP mice; Karram et al., 2008). It is worth mentioning that all these reporter mice are suitable to be combined with imaging of ion-sensitive dyes (Moshrefi-Ravasdjani et al., 2017).

A hallmark of classical astrocytes is their large K^+ conductance (Stephan et al., 2012), which results in a highly negative membrane potential (Zhou et al., 2006; Kafitz et al., 2008). Further, astrocyte properties are less

constant as the expression of many astrocyte-typical proteins is regulated during early postnatal development (Felix et al., 2020b). For example, the expression of inwardly rectifying K^+ channels ($Kir_{4.1}$) and two-pore domain K^+ channels (K_{2p}) increases (Seifert et al., 2009; Nwaobi et al., 2014; Lunde et al., 2015; Moroni et al., 2015; Olsen et al., 2015) causing a strong decrease in membrane resistance (R_M ; Zhou et al., 2006; Kafitz et al., 2008; Stephan et al., 2012; Zhong et al., 2016). Simultaneously, the detectable amount of K_V channel-mediated currents decreases, which together alters the astrocytic current-voltage relationship from non-linear to linear (Zhou et al., 2006; Kafitz et al., 2008; Zhong et al., 2016). In contrast to NG2 glia, astrocytes do not express Na_V channels (Matthias et al., 2003; Zhou et al., 2006; Kafitz et al., 2008; Zhong et al., 2016).

ANALYSIS OF GAP JUNCTIONAL COUPLING

There are many different techniques available to study gap junctions. These include but are not limited to whole-cell patch-clamp (paired recordings, analysis of isopotentiality, tracer injection), genetic approaches (FRAP, PARIS, StarTrack, transgenic mice), imaging of ion-sensitive dyes (e.g., SBFI), and expression studies (immunohistochemistry, western blotting) (Abbaci et al., 2008; Giaume and Theis, 2010; Bedner et al., 2012; Langer et al., 2012; Griemsmann et al., 2015; Droguerre et al., 2019; Eitelmann et al., 2019; Gutierrez et al., 2019; Wu et al., 2019; Du et al., 2020; McCutcheon et al., 2020). Here, we focus on approaches to analyze gap junctional communication that can be implemented easily in most electrophysiology and imaging laboratories.

Patch Clamp-Based Approaches

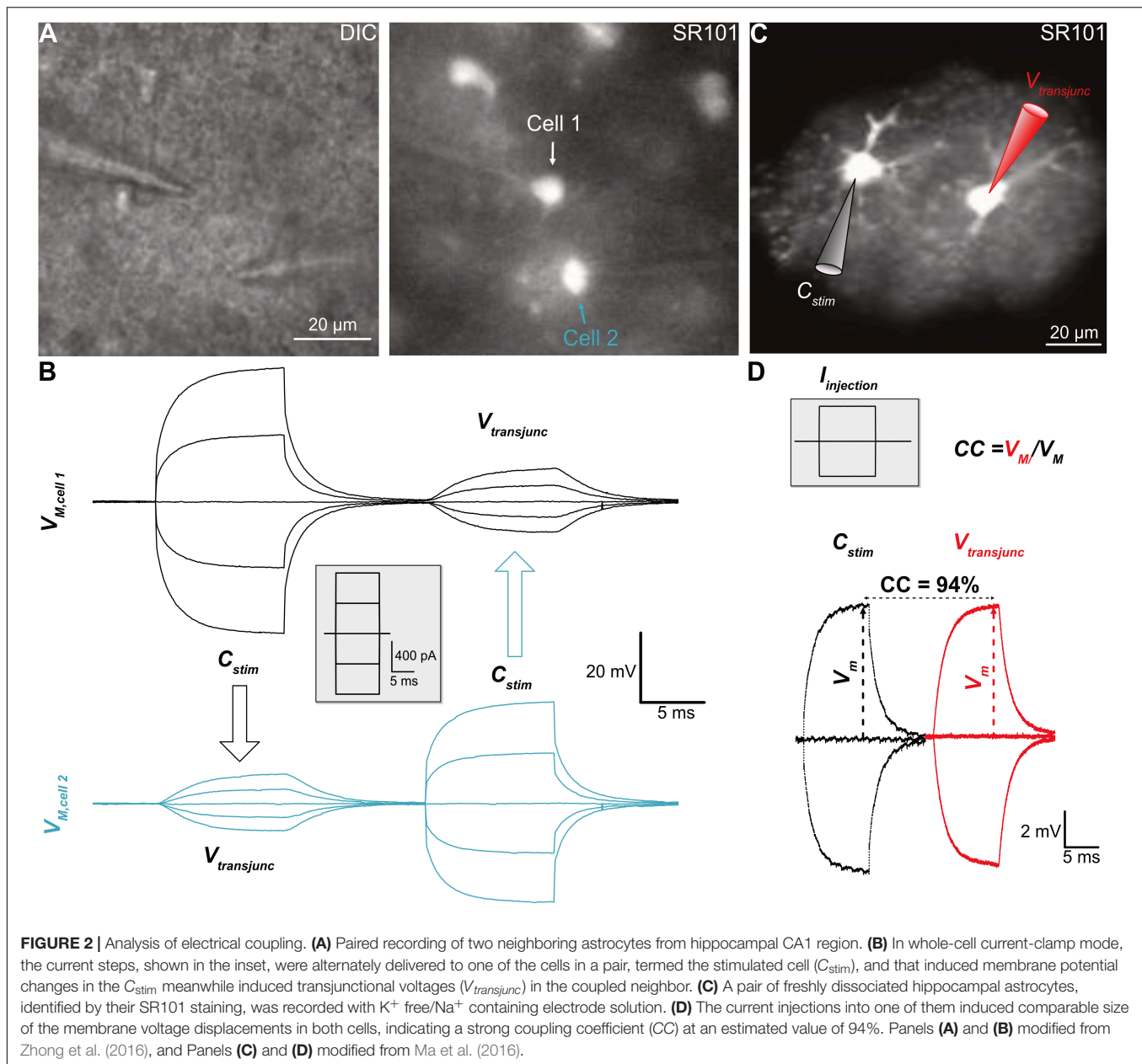
Electrophysiological methods are commonly used to detect gap junctional coupling of cells. In 1966, the first evidence that astrocytes are intercellularly coupled was provided by an electrophysiological study of amphibian optic nerve by Kuffler et al. (1966). In their report, an elegant triple-sharp-electrode recording mode was used to reveal a “low-resistance connection” between neuroglia, which we know now as the gap junctional coupling of fibrous astrocytes in optic nerves. This electrophysiological method was continually used until the 1980s for glial physiology study. For example, Kettenmann and Ransom used it to record cultured astrocytes and oligodendrocytes, confirming that gap junctions were indeed the molecular identities for the functional coupling of these glial subtypes (Kettenmann and Ransom, 1988; Ransom and Kettenmann, 1990).

The advent of patch-clamp in the 1990s ushered electrophysiological studies into a new era. Since the patch-clamp system is able for simultaneous current injection and membrane potential recording, now only two electrodes are used for paired recording. Here, we will limit our discussion to this advanced paired recording mode and its application to analyze the functional connectivity of neighboring astrocytes.

Until now, this technique has been used by several research laboratories for study of gap junctional coupling in native astrocytes in brain slices and freshly isolated astrocytes (Muller et al., 1996; Meme et al., 2009; Xu et al., 2010, 2014; Ma et al., 2016; Zhong et al., 2016; Kiyoshi et al., 2018). These studies demonstrated the paired recording mode as a highly sensitive method for revealing the functional coupling of astrocytes *in situ* and in pairs of freshly dissociated astrocytes. To address the electrical role of gap junctional coupling for astrocyte syncytium, a single electrode method was developed in 2016 with details described in the following “Astrocyte Syncytial Isopotentiality” section. Together with computational modeling, this method allows for monitoring dynamical changes in the coupling strength of an astrocyte syncytium (Ma et al., 2016; Kiyoshi et al., 2018). Another way to assess gap junctional coupling is to add a tracer to the internal solution of patch pipettes and to visualize gap junction-coupled cells. In the following section, we will first discuss the rationale, application, advantage, and limitation of the commonly used paired recording model and the newly developed syncytial isopotentiality measurement. Thereafter, we will highlight, how the addition of gap junction-permeable tracers to the pipette solution can be used to visualize cell-to-cell coupling and to subsequently analyze the topography of tracer-coupled networks.

Paired Recording Mode

The rationale behind the design of the paired recording model lies in the basic properties of gap junction channels. Gap junctions are large aqueous pores, 8–16 Å, filled with electrolytes that make them ideal electrical conductors for the flow of ionic currents between coupled cells (Weber et al., 2004). In the adjacent cells, the easiness of the ionic current flow is determined by the number of gap junctions aggregated on the plaques in the interface of the adjacent cells, or the intercellular gap junctional resistance (R_{gap}). Accordingly, the paired recording mode is designed to examine the R_{gap} through the passing of injected currents in one of the two coupled cells and to measure subsequently the size of remaining transjunctional voltage arriving at the second cell (Figures 2A,B; Bennett, 1966; Bennett et al., 1991; Ma et al., 2016). There are unique characteristics associated with paired recordings. It is known that the gap junctions formed by different Cxs differ in their permeability properties for endogenous compounds, therefore, differentially regulate the intercellular transfer of metabolites, i.e., glucose, and signaling molecules, such as ATP, glutamate, and IP_3 (Goldberg et al., 1999, 2002; Niessen et al., 2000). It is also known that Cxs vary in pore size and conductivity (~30 to ~300 pS) (Hille, 2001). However, the Cxs ubiquitously exhibit high selectivity to the major intracellular monovalent cation K^+ and Na^+ in the order of $K^+ > Na^+$ (Wang and Veenstra, 1997), and these ions are charge carriers that mediate current flow between coupled cells. Thus, independent of Cx isoforms, transjunctional voltage measurements stand out as an universal readout of gap junctional coupling (Veenstra et al., 1995; Veenstra, 1996). Additionally, paired recordings are featured by their high detection sensitivity conferred by the



state-of-the-art electronic engineering technology of the patch-clamp amplifier, allowing detection of the ionic currents at the picoampere scale.

Experimentally, two adjacent astrocytes are sequentially recorded in whole-cell mode (Figures 2A,B). Subsequently, the current can be alternately injected into one of the recorded cells, defined as the stimulated cell (C_{stim}), whereas the transjunctional voltage is recorded in the neighboring recipient cell (C_{reci}). Although the R_{gap} can be calculated from the basic membrane properties and the current-induced membrane voltages, the coupling strength is commonly expressed as the coupling coefficient (CC)—the ratio of voltages measured from the C_{reci}/C_{stim} . The higher a CC value, the stronger the cell-to-cell coupling (Bennett, 1966; Bennett et al., 1991; Ma et al., 2016).

A major advantage of paired recordings is their high sensitivity, which is determined by the open probability that is universally high among gap junctions in the range of 0.6–0.9; whereas the sensitivity of tracer coupling is mostly determined by the pore selectivity that varies among gap junctions (Nielsen et al., 2012). Consequently, in simultaneous transjunctional voltage and dye coupling measurements, it is common to see measurable transjunctional voltages in an absence of detectable dye coupling (Murphy et al., 1983; Ransom and Kettenmann, 1990; Sontheimer et al., 1991; Xu et al., 2010). An example that paired recordings have a higher sensitivity was shown in a study carried out in hippocampal astrocytes *in situ* (Xu et al., 2010). Incubation of brain slices with a gap junction inhibitor, meclofenamic acid (MFA, 100 μ M), was able to inhibit astrocyte

gap junctional coupling by 99% (Ma et al., 2016). Interestingly, in the presence of 100 μM MFA, the cross-diffusion of two tracers, Lucifer Yellow (LY) and biocytin, separately loaded into two recording electrodes, were completely inhibited, whereas the transjunctional voltages remained intact (Xu et al., 2010). In the barrel cortex, the Cx43 expression was found to be enriched within the barrels, but largely absent in the inter-barrel space (septa), and this was associated with a restricted dye coupling inside the barrels (Houades et al., 2006). To examine whether such segregated dye coupling indeed indicates a complete absence of gap junctional of astrocytes between barrels and their surrounding septa, the paired recording was carried out between a pair of astrocytes, one inside another outside of the barrel. The results showed that in the transjunctional voltage measurement, astrocytes do communicate inside and outside of the barrels and, therefore, are gap junctional coupled into a syncytium (Kiyoshi et al., 2018). Therefore, the existence of gap junctional coupling can be more sensitively inspected by this method.

Nevertheless, there are also technical challenges and limitations. First of all, still, only a handful of experimenters successfully employed paired recordings in their research. The technical complexity of paired recordings to monitor junctional coupling has limited more researchers to take advantage of this powerful tool in their glial physiology study. The second obstacle that impedes the application of paired recordings is the low R_M of astrocytes at an estimated level of 6.4 $\text{M}\Omega$ (Du et al., 2015). As a result, the “leaky” membrane shunts most of the injected currents, making it impossible to estimate the current passing through gap junctions resulting in erroneous CC calculation (Du et al., 2020). To make the matters worse, astrocytes are coupled into a syncytial network; each astrocyte is typically directly coupled to 7–9 nearest neighbors across the brain (Xu et al., 2010; Ma et al., 2016; Kiyoshi et al., 2018). Consequently, the injected currents to one of the recorded astrocytes should be redistributed into coupled astrocytes at unknown ratios (in a parallel electrical circuit) (Cotrina et al., 1998). Therefore, the leaking membrane and syncytial coupling make it next to impossible to calculate the actual CC in brain slice recordings. Consequently, rather low CC values in the range from 1.6% to 5.1% were reported from hippocampal astrocytes *in situ* (Meme et al., 2009; Xu et al., 2010).

To solve this problem, the innovative use of paired recordings was applied to freshly dissociated pairs of astrocytes to avoid extensive coupling. To circumvent the shunt of injected currents through abundantly expressed membrane K^+ channels, the physiological K^+ content in the electrode solution was substituted equimolarly by Na^+ ; hence, the electrode Na^+ equilibrating with the recorded pair of astrocytes will not leak through the membrane K^+ channels, and measured currents will therefore better reflect junctional coupling (Figures 2C,D). Under these conditions, a strong coupling CC of 94% was revealed. Based on this CC , there was an estimate of 2,000 gap junctions aggregated at the interface of two neighboring astrocytes, and a calculated R_{gap} at 4.3 $\text{M}\Omega$ (Ma et al., 2016), which is even lower than the astrocytic R_M of 6.4 $\text{M}\Omega$ (Du et al., 2015). These results together indicate that the electrical barrier between astrocytes is nearly absent. Recently, ultrastructural

details of astrocyte-astrocyte contacts have been revealed that explain how such a low inter-astrocytic resistance could be biophysically achieved (Kiyoshi et al., 2020).

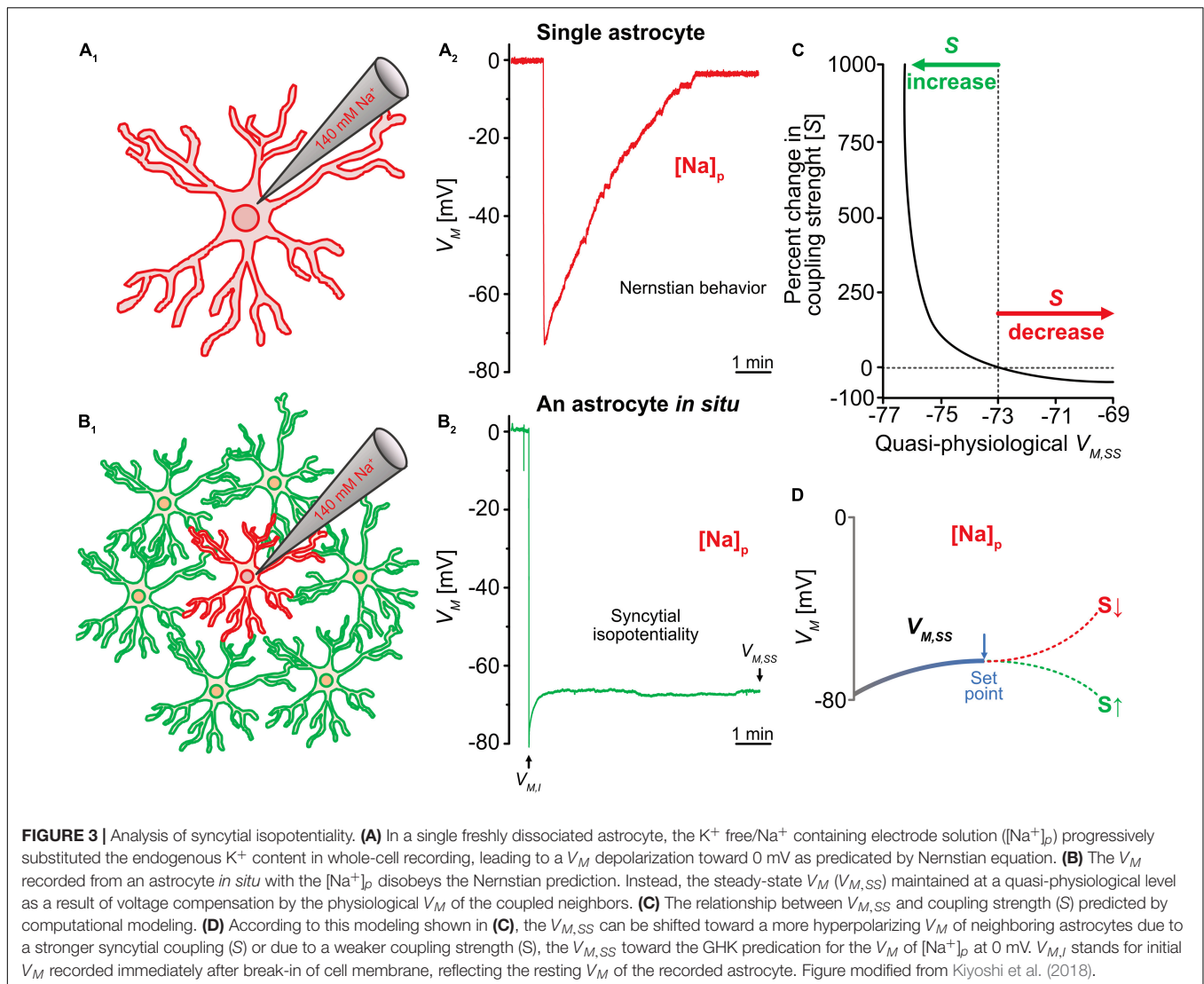
In summary, the rationale for paired recordings is based on an uniform feature of high open probability of gap junction channels for two intracellular monovalent cations, K^+ and Na^+ . Therefore, it offers a rather universal readout to study the functional gap junctional coupling at high sensitivity. For brain slice studies, however, the paired recordings are most valuable for inspecting the existence of functional gap junctional coupling, but are of limited value for quantitative analysis of the CC between astrocytes due to the low R_M and syncytial coupling. Combinatory use of freshly dissociated pairs of astrocytes and non-physiological Na^+ or Cs^+ electrode solution is a powerful alternative to circumvent the above obstacles.

Astrocyte Syncytial Isopotentiality

As mentioned above, the R_{gap} between astrocytes is even lower than astrocytes' R_M , suggesting that two neighboring astrocytes are able to constantly equalize their membrane potentials and therefore electrically behave as one cell. By extension, the gap junction coupled astrocytes should then be able to balance their membrane potentials to comparable levels so that a syncytial isopotentiality could be achieved. In fact, this possibility was postulated in the past (Muller, 1996) and was discussed by Richard Orkand and his colleagues to be a necessity for the operation of K^+ spatial buffering in the brain (personal communication with Dr. Serguei Skatchkov). This syncytial isopotentiality was experimentally demonstrated in 2016 (Ma et al., 2016), and a system-wide existence of this feature in the astrocyte networks was confirmed soon after that (Huang et al., 2018; Kiyoshi et al., 2018; Wang W. et al., 2020).

The rationale for the methodological design is based on a basic feature of astrocytes. Physiologically, an astrocyte behaves as a perfect K^+ electrode (Kuffler et al., 1966; Ransom and Goldring, 1973). Therefore, one can experimentally substitute the intracellular K^+ concentration ($[\text{K}^+]_i$) through dialysis of the recorded cell with electrode solution containing equimolar (i.e. 140 mM) Na^+ (or Cs^+) (Ma et al., 2016; Wang W. et al., 2020). This, in turn, alters the V_M of the recorded astrocyte from K^+ equilibrium potential (E_K , -80 mV) to Na^+ equilibrium potential (E_{Na} , ~ 0 mV) according to the prediction from the Goldman-Hodgkin-Katz (GHK) equation. In single freshly dissociated astrocytes, the V_M indeed shifts to ~ 0 mV (Figure 3A) (Kiyoshi et al., 2018). However, should the R_{gap} be sufficiently low, the associated syncytium can then instantaneously act to compensate for the loss of physiological membrane potential (V_M) in the recorded cell, and the level of the compensation should be determined by the coupling strength and the number of directly nearest coupled neighbors (Ma et al., 2016; Kiyoshi et al., 2018).

Experimentally, the syncytial isopotentiality can be detected by the substitution of endogenous K^+ by a 140 mM Na^+/K^+ -free electrode solution ($[\text{Na}^+]_p$) (Figures 3A,B) and recording the astrocyte in current-clamp mode. The breakthrough of the membrane patch shifted the V_M immediately to a resting membrane potential of -78 mV (Figures 3A,B). Over time, the V_M reaches a stationary level of -73 mV. This is in sharp contrast to the anticipated depolarization to 0 mV as predicted by the



GHK equation for K^+ -free electrode solution (**Figure 3A**). The initial V_M recording ($V_{M,I}$) reflects the true resting V_M of an astrocyte (Ma et al., 2016; Kiyoshi et al., 2018). In hippocampal astrocyte syncytium, the steady-state V_M ($V_{M,SS}$) in $[Na^+]_p$ recordings is ~ 5 mV more depolarized than $V_{M,I}$.

The Ionic Mechanisms Engaged in the Establishment of $V_{M,SS}$

To biophysically explain how the quasi-physiological $V_{M,SS}$ is established, different size of syncytia, i.e., syncytia containing varying number of astrocytes, were used for $V_{M,SS}$ recordings, and computational modeling was used to simulate the underlying ionic mechanisms (Ma et al., 2016). The rupture of an astrocyte with $[Na^+]_p$ initiates dialysis of Na^+ to the recorded astrocyte and associated syncytium (**Figure 3B1**). In the recorded cell, the Na^+ dialysis dissipates the endogenous K^+ content hence abolishes the physiological V_M established by the across membrane K^+ gradient. To the coupled syncytium, the Na^+ dialysis generates a Na^+ gradient and current flow

across gap junctions that depolarizes neighboring astrocytes and hyperpolarizes the recorded cell. The latter is the major contributor to the quasi-physiological $V_{M,SS}$. Additionally, the dissipation of K^+ content in the recorded cell attracts an influx of K^+ from neighboring astrocytes. The accumulated K^+ has the potential to establish a hyperpolarizing potential in the recorded cell therefore additionally contributes to the totality of the quasi-physiological $V_{M,SS}$ (Ma et al., 2016). As shown in **Figure 3B2**, these two ionic flows take approximately 5 min to reach a steady-state after rupture of whole-cell recording (**Figure 3B2**).

How does the strength of syncytial isotopotentiality influence the intensity of the Na^+ and K^+ current flows? As noted above, in the $[Na^+]_p$ recorded astrocyte, there are two ionic current flows in opposite directions and collectively contribute to the measured $V_{M,SS}$; the outward-going Na^+ current from recorded cell to the coupled cells, and inward-going K^+ current flow from the coupled astrocytes to the recorded cell. To simplify the analysis, we take the outward-going Na^+ ($I_{Na,out}$) to one of the coupled astrocytes as an example, the proximity of the potentials

in these two cells can be expressed as the difference of the voltages between the Na⁺-loaded astrocyte (V_{Na}) and a coupled neighbor (V_N)

$$(V_N - V_{Na}) = R_{\text{gap}} * I_{\text{Na,out}}$$

where $(V_N - V_{Na}) = 0$ mV is a theoretically ideal isopotentiality achieved between the two cells. Assuming $I_{\text{Na,out}}$ is a constant determined by its chemical gradient down the neighboring cell, then a higher strength of isopotentiality, i.e., lower $(V_N - V_{Na})$, is correlated to a lower junctional resistance (R_{gap}). Secondly, as $(V_N - V_{Na})$ approaches the ideal isopotentiality of 0 mV, the $I_{\text{Na,out}}$ also diminishes to ~ 0 pA. By extension, closer proximity of potentials between the recorded cell and its associated astrocytes, the less outward-going Na⁺ current flow from $[\text{Na}^+]_p$ recorded astrocyte toward its associated syncytium.

Likewise, the intensity of the inward-going K⁺ current ($I_{\text{K,in}}$) and syncytial coupling strength follows with the same relationship:

$$(V_N - V_{Na}) = R_{\text{gap}} * I_{\text{K,in}}$$

where the inward-going K⁺ current is impeded by increasing proximity of the V_{Na} to V_N . It should be noted that K⁺ cannot be substantially buildup due to efflux of K⁺ through membrane K⁺ channels in the $[\text{Na}^+]_p$ recorded astrocyte; consequently, less hyperpolarizing potential can be built up to make a significant contribution to the recorded $V_{M,SS}$.

In summary, we described a method that uses $[\text{Na}^+]_p$ to disrupt the continuity of a syncytial isopotentiality, and that in turn informs of the existence and the strength of the isopotentiality in an astrocyte syncytium. Biophysically, gap junctional ionic movement occurs during the equalization of the potential differences in a syncytium, therefore a strong syncytial isopotentiality means a less ionic movement inside a syncytium. Additionally, a larger syncytium has a greater capacity to minimize the ionic movement, which has been simulated in a computational model (Ma et al., 2016). Functionally, in the event of local extracellular environment changes, e.g., neuronal firing induced high K⁺, syncytial isopotentiality provides a sustained driving force to individual astrocytes for high efficient K⁺ uptake, spatial transfer and release of K⁺ to regions where neuronal activity is low (Terman and Zhou, 2019).

V_{M,SS} as a Functional Readout of Coupling Strength (S) of Syncytial Coupling

Based on the discussion above, the $V_{M,SS}$ is established and regulated by the R_{gap} and the number of astrocytes in a coupled syncytium, therefore can lean to a more hyperpolarizing V_M in the neighboring astrocytes, or a more depolarizing V_M established by intracellular Na⁺. Thus, the $V_{M,SS}$ serves as a dynamic readout of the strength of syncytial coupling. To be able to quantitatively correlate the changes of $V_{M,SS}$ with S, a computational model has been established (Figures 3C,D) where a stronger syncytial coupling leads to a stronger compensation of the $V_{M,SS}$ towards the physiological V_M of neighboring astrocytes established by

140 mV $[\text{K}^+]_i$, whereas a weaker coupling shifts the $V_{M,SS}$ toward GHK predicted E_K for the Na⁺ electrode solution. More details about the biophysical principles and assumptions used to build up this computational model are available in this publication (Kiyoshi et al., 2018). In addition, this model can be used for analysis of the dynamic change of coupling strength, for instance, during neuronal activation (Kiyoshi et al., 2018).

This method comprises several advantages. First, differing from paired recordings, $V_{M,SS}$ is measured from single electrode recordings. Second, this method allows for dynamic monitoring of the coupling strength of a syncytium over time. Third, this method can be incorporated with astrocyte syncytial anatomy studies. For example, ALDH1L1-eGFP reporter mice were used for *a priori* astrocyte identification and examination of syncytial isopotentiality across brain regions. Additionally, the recorded brain slices were then further processed with the tissue-clearing method (Susaki et al., 2014, 2015), i.e., depletion of the brain lipid content, for high-resolution confocal imaging study of the cellular morphology and spatial organization patterns of astrocytes (Kiyoshi et al., 2018). This study showed that in different layers of the visual cortex, the anatomy, in terms of cell density, interastrocytic distance and the number of the nearest neighbors vary in morphometric analysis. However, S does not differ between layers. Additionally, S of the visual cortex was found to be stronger than in the hippocampal CA1 region (Kiyoshi et al., 2018). Fourthly, this method can be incorporated with tracer coupling to map the directionality and spatial coupling of a syncytium (see also “Tracer Coupling”). For example, in the cerebellum, Bergmann glia and velate astrocytes are derived from the same progenitor pool but are strikingly different in their morphology (Kita et al., 2013). Bergmann glia are characterized by having their cell bodies arranged in rows alongside with the soma of Purkinje neurons and extension of their processes along the Purkinje cell layer toward the *pia* of the cerebellum. Velate astrocytes are cerebellar protoplasmic astrocytes that exhibit characteristic velate sheath processes and are more dispersed in arrangement (Chan-Palay and Palay, 1972). S is significantly weaker in Bergmann glia networks than those established by velate astrocytes at the granular layer. In the tracer coupling analysis, the injection of tracer revealed the coupling of Bergmann glia and velate astrocytes. Thus, despite a striking difference in syncytial anatomy, the syncytial isopotentiality occurs to syncytial networks established by both subtypes of astrocytes (Kiyoshi et al., 2018).

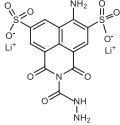
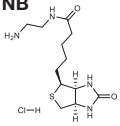
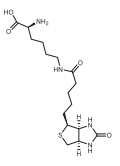
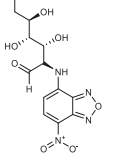
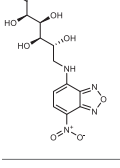
A limitation in this method is the inference of a syncytial isopotentiality based on biophysical principles and electrophysiological measurements. Significant progress has been made in the technique of genetically encoded voltage indicator (Kang et al., 2019). However, this state-of-the-art technique is still below the threshold to detect the subtle variation of voltages in an astrocyte syncytium, and therefore, future optimization of this technique is crucial to recruit advanced imaging techniques to study the physiology and pathology of astrocyte syncytial networks.

Tracer Coupling

Aside this direct measurement of cell-to-cell coupling, tracer coupling can be utilized to mimic diffusion within the network. Tracers are usually loaded for several minutes into a single cell via the backfill of the patch pipette. Simultaneously, tracers diffuse within the gap junction network. The tracer concentration is highest in the patched cell and declines within the network with increasing distance as it diffuses. There are various tracers available comprising different advantages and disadvantages (Table 1; see also Abbaci et al., 2008). An often used tracer is LY (Kawata et al., 1983). It is a fluorescent dye that allows direct observation of diffusion within the network. Subsequently, LY labeling can be combined with immunohistochemistry to determine the identity of coupled cells (Binmoller and Muller, 1992; Konietzko and Muller, 1994). However, it comprises low permeability at gap junctions consisting of Cx30 (Rackauskas et al., 2007). As Cx30 expression increases during early postnatal development (Nagy et al., 1999; Griemsmann et al., 2015; Augustin et al., 2016; Wadle et al., 2018), LY will only highlight a fraction of coupling in more mature tissue. In addition, LY has

a low solubility and tends to clog electrodes. As LY interferes with endogenous electrophysiological properties, it is rather not suitable to be combined with electrophysiological analyses (Tasker et al., 1991). Further fluorophores, e.g., Alexa Fluor (AF) dyes, can be used for tracing coupled cells as well (Han et al., 2013). Like LY, spreading of AF dyes can be assessed directly. However, they do not pass through Cx30 containing gap junctions and just insufficiently through other gap junctions requiring administration at high concentration (Weber et al., 2004). At lower concentrations, there is almost no diffusion to neighboring cells so that AF dyes can be used to label the patch-clamped cell (Augustin et al., 2016; Wadle et al., 2018; Eitelmann et al., 2019). Two other tracers, namely neurobiotin (Nb) and biocytin (Horikawa and Armstrong, 1988; Huang et al., 1992), are colorless and require fixation and further processing of the tissue. Thus, their diffusion cannot be assessed directly. The two tracers are recognized by streptavidin and avidin (Livnah et al., 1993). The latter ones can be linked to either fluorophores or enzymes. Using a fluorophore allows the combination with further immunohistochemical processing of the tissue (Schools

TABLE 1 | Commonly used tracers for analyzing gap junctional coupling.

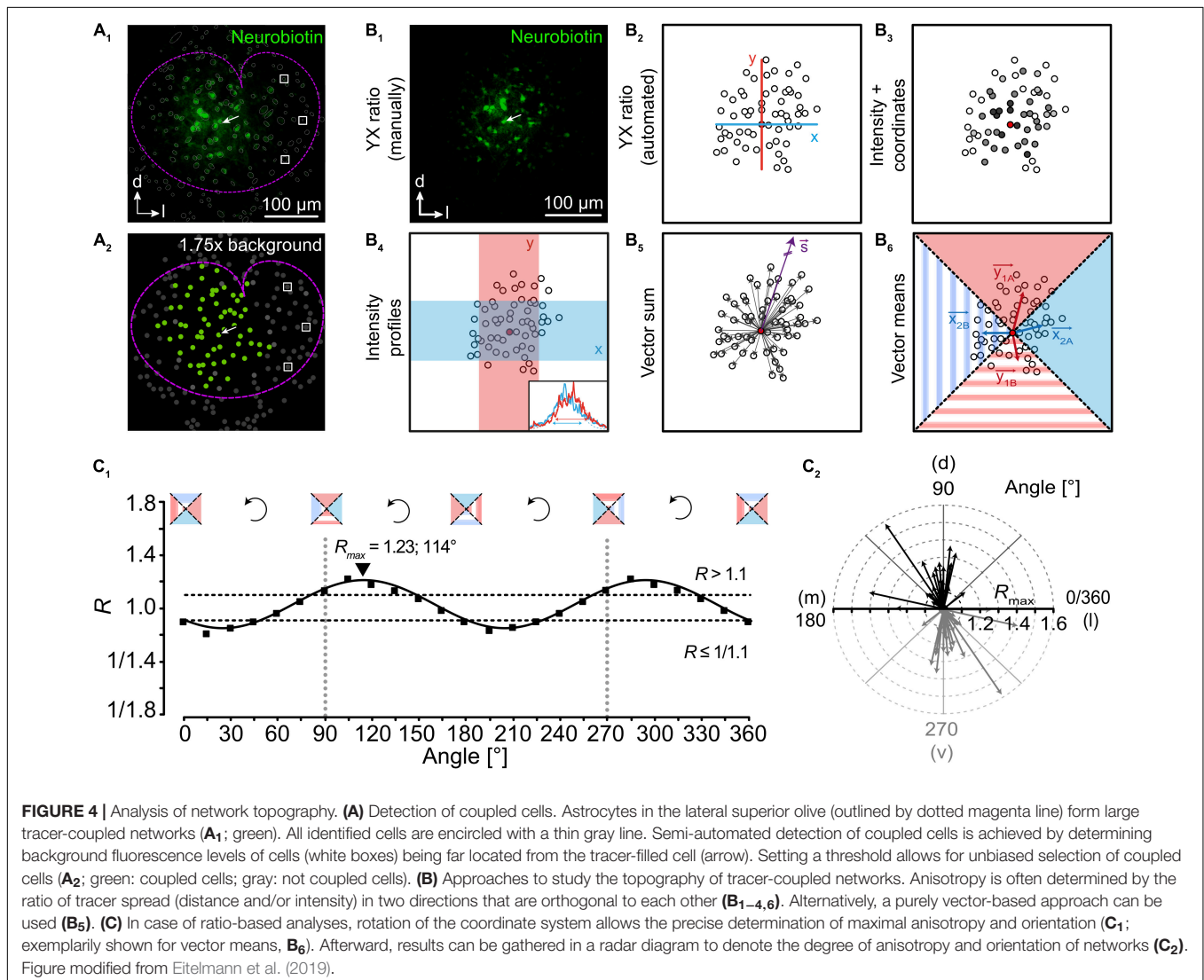
Tracer	Mass [g/mol]	Fluorescence	Histology required	Advantage	Disadvantage	Reference(s)
LY 	457	✓	✗	Direct imaging	Low Cx30-permeability Alteration of electrophysiological properties	Tasker et al., 1991 Kawata et al., 1983 Rackauskas et al., 2007
NB 	323	✗	(Strept-/) Avidin conjugates	Permeable through all astrocytic Cx	Background labeling of endogenous biotin	Huang et al., 1992 Livnah et al., 1993
Biocytin 	375	✗	(Strept-/) Avidin conjugates	Permeable through all astrocytic Cx	Background labeling of endogenous biotin	Horikawa and Armstrong, 1988 Livnah et al., 1993
2-NBDG 	342	✓	✗	Imaging of glucose distribution	Degradation to non-fluorescent derivative	Yoshioka et al., 1996 Yamada et al., 2000
6-NBDG 	342	✓	✗	Imaging of glucose distribution		Speizer et al., 1985

LY, Lucifer Yellow; NB, neurobiotin; Cx, connexin; NBDG, deoxy-N-(7-nitrobenz-2-oxa-1,3-diazol-4-yl)-aminoglucose; AF, Alexa Fluor.

et al., 2006; Augustin et al., 2016; Eitelmann et al., 2019, 2020). Using peroxidases produces a light-stable product that is not sensitive to photo-bleaching (Konietzko and Muller, 1994; D'Ambrosio et al., 1998). Alternatively, fluorescent glucose analogues can be used (Speizer et al., 1985; Yamada et al., 2000). They allow to visualize activity-dependent, directed glucose redistribution in otherwise spherical networks (Rouach et al., 2008). However, it has to be kept in mind that, for example, 2-NBDG enters the glycolytic pathway and is degraded to a non-fluorescent derivative (Yoshioka et al., 1996).

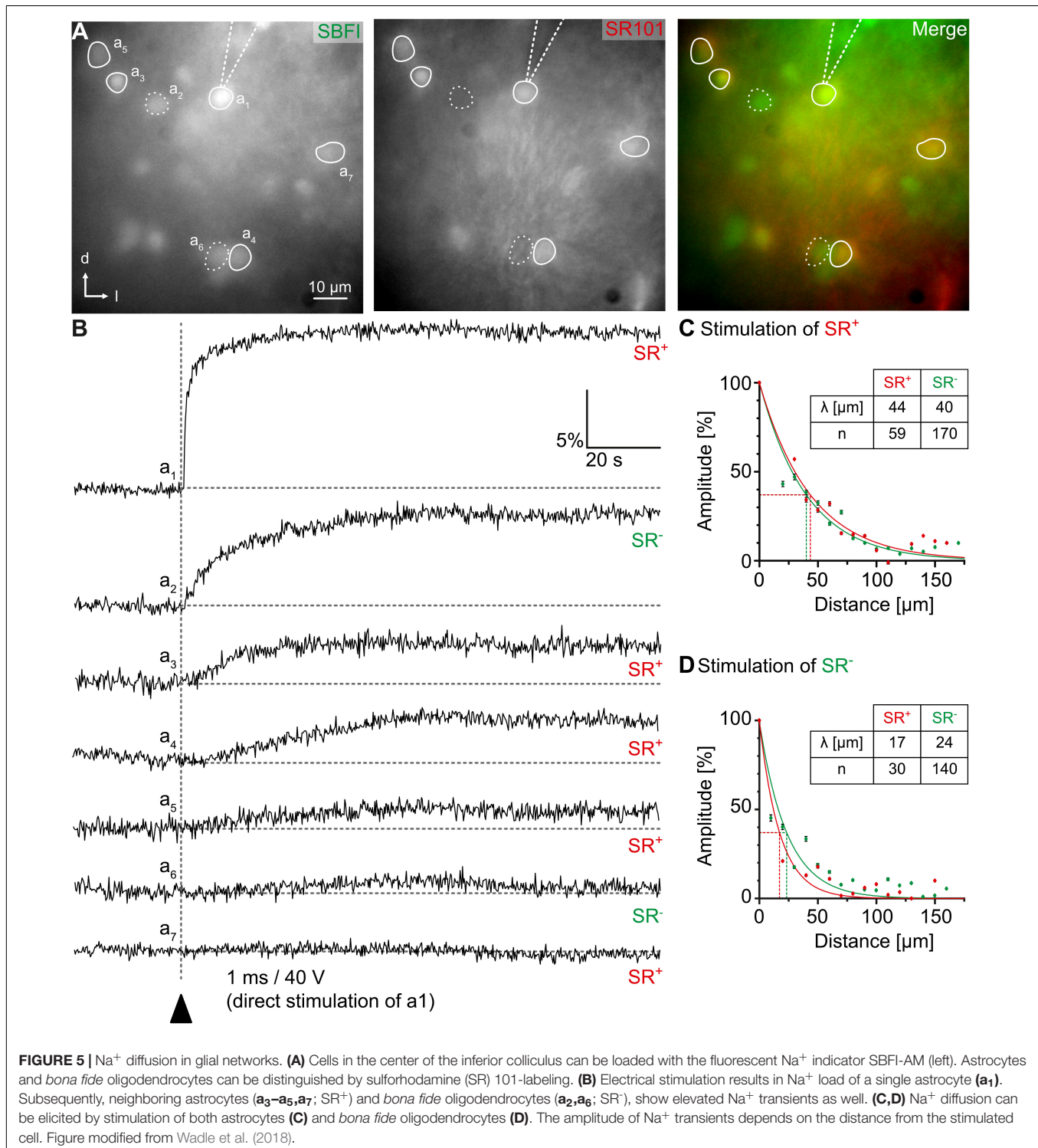
Gap junctional coupling is not uniform, e.g., it was shown to increase developmentally (Binmoller and Muller, 1992; Schools et al., 2006; Houades et al., 2008; Langer et al., 2012; Griemsmann et al., 2015). Furthermore, there are many examples of spherical networks upon radial tracer diffusion in certain brain regions (Binmoller and Muller, 1992; Houades et al., 2006; Muller et al., 2009). However, in others—in particular in sensory systems—tracer spreading is unequal in different directions (Houades et al., 2008; Augustin et al., 2016; Claus et al., 2018; Condamine

et al., 2018a; Wadle et al., 2018). There, network anisotropy strongly correlates with anatomical and functional organization of the underlying neuronal circuitry. The anisotropy of tracer spreading originates from astrocyte topography (Anders et al., 2014; Augustin et al., 2016; Ghezali et al., 2018; Wadle et al., 2018). Interestingly, in the lateral superior olive—a conspicuous nucleus in the auditory brainstem—absence of spontaneous cochlea-driven neuronal activity leading to disturbed neuronal circuitry (Hirtz et al., 2012; Muller et al., 2019) causes altered astrocyte topography followed by altered orientation of tracer-coupled networks (Eitelmann et al., 2020). In recent years, several different approaches were developed to analyze the anisotropy of tracer-coupled networks (Figure 4). Most approaches are able to reliably detect network anisotropy; however, some are working only in certain brain regions (Eitelmann et al., 2019). The different approaches rely on (1) distance of the farthest cells that are labeled, (2) labeling intensity, (3) position of all coupled cells, or (4) a combination of the aforementioned parameters. Most approaches use the ratio of the diffusion range and/or brightness



of the tracer in two directions. The most convenient approach is to measure the extent of tracer spreading in two directions orthogonal to each other (“YX ratio”). Here, anisotropy is determined by the four outermost cells showing tracer signal (Figure 4B_{1,2}; Houades et al., 2006, 2008; Augustin et al., 2016; Ghezali et al., 2018; Wadle et al., 2018). However, since the

tracer signal is declining with distance to the loaded cell, it can be difficult to determine the correct extension of the network. Alternatively, the product of network extension multiplied with the somatic tracer intensity for two directions orthogonal to each other can be calculated (“Intensity + coordinates”; Figure 4B₃; Anders et al., 2014). However, elevated somatic signal intensities



due to expression of endogenous biotin (Bixel and Hamprecht, 2000; Yagi et al., 2002) might result in a distorted ratio. In another approach, the labeling intensity of somata and processes is analyzed to determine network anisotropy (“Intensity profiles”; **Figure 4B₄**; Claus et al., 2018). Here, intensity plot profiles of two rectangles orthogonal to each other and the ratio of respective full-width at half-maximum (FWHM) are calculated. However, cell number or individual positions are neglected and must be analyzed separately, if required. Finally, there are two vector-based approaches. The first calculates the “Vector sum” (**Figure 4B₅**; Condamine et al., 2018a,b). However, it only works in brain regions with defined borders, i.e., diffusion barriers resulting from reduced gap junction coupling. Examples of such brain regions are the trigeminal main sensory nucleus and the columns of the barrel cortex. In both, gap junction coupling is stronger within the nucleus and columns compared to areas outside. However, anisotropic tracer diffusion will be visualized only if the tracer is injected into an astrocyte that is not located in the center (Houades et al., 2008; Condamine et al., 2018a) as the “Vector sum” approach is not capable to detect the anisotropy of tracer-coupled networks if they are symmetric with respect to a point (Eitelmann et al., 2019). The second vector-based approach calculates the “Vector means” in four 90° sectors and the ratio of tracer extension is calculated (**Figure 4B₆**; Eitelmann et al., 2019, 2020). However, analyzing the anisotropy of tracer spreading using only two fixed axes might result in falsified results. For example, if an anisotropic network is turned by 45° from one of the two axes, all ratio-based approaches will postulate spherical network. Therefore, a subsequent analysis using a rotating coordinate system will not only determine the maximal anisotropy of a network, but will also define the preferred orientation (**Figure 4C**; Eitelmann et al., 2019). Taken together, heterogeneity of gap junctional coupling can be visualized excellently by tracer coupling studies. However, they often provide only a snap-shot of coupling using a non-physiological tracer.

Wide Field (Na⁺) Imaging

Imaging of intracellular ion concentration can be a good tool to supplement tracer coupling studies. For the interpretation of ion diffusion within the gap junction network, it is beneficial to analyze the spread of ions that is less effected by signaling cascades. Thus, Ca²⁺ is a less suitable candidate as signaling to neighboring cells is generated by intra- and extracellular pathways (Giaume and Venance, 1998; Bernardinelli et al., 2004; Scemes and Giaume, 2006). However, intercellular Na⁺ spread depends on gap junctional coupling as deletion of Cx43 and Cx30 prevents ion exchange between neighboring astrocytes (Wallraff et al., 2006; Langer et al., 2012). However, it has to be kept in mind that intracellular Na⁺ is not completely independent from signaling cascades as it is linked to Ca²⁺ via the Na⁺/Ca²⁺ exchanger (Felix et al., 2020a). For Na⁺ imaging, cells are dyed, e.g., with the membrane-permeable form of SBFI (SBFI-acetoxymethyl ester). After cleavage by endogenous esterases SBFI allows ratiometric imaging of [Na⁺]_i (**Figure 5**; Minta and Tsien, 1989; Meier et al., 2006). Na⁺ load into a single cell can be achieved via direct electrical stimulation. This will result in

Na⁺ rise in the stimulated and in neighboring cells (**Figure 5B**; Langer et al., 2012; Augustin et al., 2016; Moshrefi-Ravasdjani et al., 2017; Wadle et al., 2018). Measuring the maximal [Na⁺]_i increase allows for the calculation of the length constant λ using a mono-exponential function (**Figures 5C,D**; Augustin et al., 2016; Moshrefi-Ravasdjani et al., 2017; Wadle et al., 2018), which demonstrates, how efficient Na⁺ is redistributed and how strong gap junctional coupling is. It was shown that spatial spread of Na⁺ between astrocytes was halfway far in the corpus callosum compared to other brain regions, i.e., hippocampus, lateral superior olive, and inferior colliculus (Langer et al., 2012; Augustin et al., 2016; Moshrefi-Ravasdjani et al., 2017; Wadle et al., 2018). Furthermore, Na⁺ diffusion is stronger within homocellular networks. In contrast, in heterocellular (panglial) networks Na⁺ redistribution is reduced (**Figure 5D**; Moshrefi-Ravasdjani et al., 2017; Wadle et al., 2018), which likely results from a lower permeability of connexons, which are incorporated into the heterotypic gap junction channels (Bedner et al., 2006). Taken together, imaging of ion sensitive dyes is a good supplement to tracer coupling studies to further characterize gap junctional communication.

CONCLUSION

Gap junctional communication between glial cells is important for ion and neurotransmitter homeostasis and ensures stabilization of their membrane potential. Though astrocytes throughout the brain share similar properties, they exhibit a considerable amount of region-dependent heterogeneity. To unravel these particular differences suitable approaches are necessary. In this review, we summarized and described well-established and recently developed methods that will allow electrophysiology and imaging laboratories to analyze gap junctional coupling in acute tissue slices.

AUTHOR CONTRIBUTIONS

JS and MZ designed the study. JS, MZ, and SE wrote the manuscript. SE designed and arranged the figures. All authors contributed to the article and approved the submitted version.

FUNDING

This study was supported by grants from the German Research Foundation (DFG Priority Program 1608 “Ultrafast and temporally precise information processing: Normal and dysfunctional hearing”: STE 2352/2-1) to JS and the National Institute of Neurological Disorders and Stroke (RO1NS116059) to MZ.

ACKNOWLEDGMENTS

We acknowledge the support by the Heinrich Heine University Duesseldorf.

REFERENCES

- Aasen, T., Johnstone, S., Vidal-Brime, L., Lynn, K. S., and Koval, M. (2018). Connexins: synthesis, post-translational modifications, and trafficking in health and disease. *Int. J. Mol. Sci.* 19:1296. doi: 10.3390/ijms19051296
- Abbaci, M., Barberi-Heyob, M., Blondel, W., Guillemin, F., and Didelon, J. (2008). Advantages and limitations of commonly used methods to assay the molecular permeability of gap junctional intercellular communication. *Biotechniques* 45, 56–62.
- Anders, S., Minge, D., Griemsmann, S., Herde, M. K., Steinhauser, C., and Henneberger, C. (2014). Spatial properties of astrocyte gap junction coupling in the rat hippocampus. *Philos. Trans. R. Soc. Lond. B Biol. Sci.* 369:20130600. doi: 10.1098/rstb.2013.0600
- Augustin, V., Bold, C., Wadle, S. L., Langer, J., Jabs, R., Philippot, C., et al. (2016). Functional anisotropic panglial networks in the lateral superior olive. *Glia* 64, 1892–1911. doi: 10.1002/glia.23031
- Axelsen, L. N., Calloe, K., Holstein-Rathlou, N. H., and Nielsen, M. S. (2013). Managing the complexity of communication: regulation of gap junctions by post-translational modification. *Front. Pharmacol.* 4:130. doi: 10.3389/fphar.2013.00130
- Bedner, P., Dupper, A., Huttmann, K., Muller, J., Herde, M. K., Dublin, P., et al. (2015). Astrocyte uncoupling as a cause of human temporal lobe epilepsy. *Brain* 138, 1208–1222. doi: 10.1093/brain/aww067
- Bedner, P., Niessen, H., Odermatt, B., Kretz, M., Willecke, K., and Harz, H. (2006). Selective permeability of different connexin channels to the second messenger cyclic AMP. *J. Biol. Chem.* 281, 6673–6681. doi: 10.1074/jbc.m511235200
- Bedner, P., Steinhauser, C., and Theis, M. (2012). Functional redundancy and compensation among members of gap junction protein families? *Biochim. Biophys. Acta* 1818, 1971–1984. doi: 10.1016/j.bbame.2011.10.016
- Bennett, M. V. (1966). Physiology of electrotonic junctions. *Ann. N. Y. Acad. Sci.* 137, 509–539. doi: 10.1111/j.1749-6632.1966.tb50178.x
- Bennett, M. V., Barrio, L. C., Bargiello, T. A., Spray, D. C., Hertzberg, E., and Saez, J. C. (1991). Gap junctions: new tools, new answers, new questions. *Neuron* 6, 305–320. doi: 10.1016/0896-6273(91)90241-q
- Bernardinelli, Y., Magistretti, P. J., and Chatton, J. Y. (2004). Astrocytes generate Na⁺-mediated metabolic waves. *Proc. Natl. Acad. Sci. U.S.A.* 101, 14937–14942. doi: 10.1073/pnas.0405315101
- Binmoller, F. J., and Muller, C. M. (1992). Postnatal development of dye-coupling among astrocytes in rat visual cortex. *Glia* 6, 127–137. doi: 10.1002/glia.440060207
- Bixel, M. G., and Hamprecht, B. (2000). Immunocytochemical localization of beta-methylcrotonyl-CoA carboxylase in astroglial cells and neurons in culture. *J. Neurochem.* 74, 1059–1067. doi: 10.1046/j.1471-4159.2000.0741059.x
- Breithausen, B., Kautzmann, S., Boehlen, A., Steinhauser, C., and Henneberger, C. (2020). Limited contribution of astroglial gap junction coupling to buffering of extracellular K⁽⁺⁾ in CA1 stratum radiatum. *Glia* 68, 918–931. doi: 10.1002/glia.23751
- Bukauskas, F. F., and Verselis, V. K. (2004). Gap junction channel gating. *Biochim. Biophys. Acta* 1662, 42–60.
- Cahoy, J. D., Emery, B., Kaushal, A., Foo, L. C., Zamanian, J. L., Christopherson, K. S., et al. (2008). A transcriptome database for astrocytes, neurons, and oligodendrocytes: a new resource for understanding brain development and function. *J. Neurosci.* 28, 264–278. doi: 10.1523/jneurosci.4178-07.2008
- Chan-Palay, V., and Palay, S. L. (1972). The form of velate astrocytes in the cerebellar cortex of monkey and rat: high voltage electron microscopy of rapid Golgi preparations. *Z. Anat. Entwicklungsgesch.* 138, 1–19. doi: 10.1007/bf00519921
- Chaturvedi, R., Reddig, K., and Li, H. S. (2014). Long-distance mechanism of neurotransmitter recycling mediated by glial network facilitates visual function in *Drosophila*. *Proc. Natl. Acad. Sci. U.S.A.* 111, 2812–2817. doi: 10.1073/pnas.1323714111
- Claus, L., Philippot, C., Griemsmann, S., Timmermann, A., Jabs, R., Henneberger, C., et al. (2018). Barreloid borders and neuronal activity shape panglial gap junction-coupled networks in the mouse thalamus. *Cereb. Cortex* 28, 213–222.
- Condamine, S., Lavoie, R., Verdier, D., and Kolta, A. (2018a). Functional rhythmic domains defined by astrocytic networks in the trigeminal main sensory nucleus. *Glia* 66, 311–326. doi: 10.1002/glia.23244
- Condamine, S., Verdier, D., and Kolta, A. (2018b). Analyzing the size, shape, and directionality of networks of coupled astrocytes. *J. Vis. Exp.* 4, 58116. doi: 10.3791/58116
- Cotrina, M. L., Kang, J., Lin, J. H., Bueno, E., Hansen, T. W., He, L., et al. (1998). Astrocytic gap junctions remain open during ischemic conditions. *J. Neurosci.* 18, 2520–2537. doi: 10.1523/jneurosci.18-07-02520.1998
- Cruz, N. F., Ball, K. K., and Diemel, G. A. (2007). Functional imaging of focal brain activation in conscious rats: impact of [(14)C]glucose metabolite spreading and release. *J. Neurosci. Res.* 85, 3254–3266. doi: 10.1002/jnr.21193
- Dahl, E., Manthey, D., Chen, Y., Schwarz, H. J., Chang, Y. S., Lalley, P. A., et al. (1996). Molecular cloning and functional expression of mouse connexin-30, a gap junction gene highly expressed in adult brain and skin. *J. Biol. Chem.* 271, 17903–17910. doi: 10.1074/jbc.271.30.17903
- D'Ambrosio, R., Wenzel, J., Schwartzkroin, P. A., Mckhann, G. M. II, and Janigro, D. (1998). Functional specialization and topographic segregation of hippocampal astrocytes. *J. Neurosci.* 18, 4425–4438. doi: 10.1523/jneurosci.18-12-04425.1998
- Droguerre, M., Tsurugizawa, T., Duchene, A., Portal, B., Guiard, B. P., Deglon, N., et al. (2019). A new tool for in vivo study of astrocyte connexin 43 in brain. *Sci. Rep.* 9:18292.
- Du, Y., Kiyoshi, C. M., Terman, D., and Zhou, M. (2020). “Analysis of the functional states of an astrocyte syncytium,” in *Basic Neurobiology Techniques*, ed. N. Wright (New York, NY: Humana), 285–313. doi: 10.1007/978-1-4939-9944-6_12
- Du, Y., Ma, B., Kiyoshi, C. M., Alford, C. C., Wang, W., and Zhou, M. (2015). Freshly dissociated mature hippocampal astrocytes exhibit passive membrane conductance and low membrane resistance similarly to syncytial coupled astrocytes. *J. Neurophysiol.* 113, 3744–3750. doi: 10.1152/jn.00206.2015
- Egawa, K., Yamada, J., Furukawa, T., Yanagawa, Y., and Fukuda, A. (2013). Cl(-) homeodynamics in gap junction-coupled astrocytic networks on activation of GABAergic synapses. *J. Physiol.* 591, 3901–3917. doi: 10.1113/jphysiol.2013.257162
- Eitelmann, S., Hirtz, J. J., and Stephan, J. (2019). A vector-based method to analyze the topography of glial networks. *Int. J. Mol. Sci.* 20:2821. doi: 10.3390/ijms20112821
- Eitelmann, S., Petersilie, L., Rose, C. R., and Stephan, J. (2020). Altered gap junction network topography in mouse models for human hereditary deafness. *Int. J. Mol. Sci.* 21:7376. doi: 10.3390/ijms21197376
- Eng, L. F., Ghirnikar, R. S., and Lee, Y. L. (2000). Glial fibrillary acidic protein: GFAP-thirty-one years (1969-2000). *Neurochem. Res.* 25, 1439–1451.
- Felix, L., Delekate, A., Petzold, G. C., and Rose, C. R. (2020a). Sodium fluctuations in astroglia and their potential impact on astrocyte function. *Front. Physiol.* 11:871. doi: 10.3389/fphys.2020.00871
- Felix, L., Stephan, J., and Rose, C. R. (2020b). Astrocytes of the early postnatal brain. *Eur. J. Neurosci.* [Epub ahead of print]. doi: 10.1111/ejn.14780
- Fuss, B., Mallon, B., Phan, T., Ohlemeyer, C., Kirchhoff, F., Nishiyama, A., et al. (2000). Purification and analysis of in vivo-differentiated oligodendrocytes expressing the green fluorescent protein. *Dev. Biol.* 218, 259–274. doi: 10.1006/dbio.1999.9574
- Ghezali, G., Calvo, C. F., Pillet, L. E., Lense, F., Ezan, P., Pannasch, U., et al. (2018). Connexin 30 controls astroglial polarization during postnatal brain development. *Development* 145:dev155275. doi: 10.1242/dev.155275
- Ghirardini, E., Wadle, S. L., Augustin, V., Becker, J., Brill, S., Hammerich, J., et al. (2018). Expression of functional inhibitory neurotransmitter transporters GlyT1, GAT-1, and GAT-3 by astrocytes of inferior colliculus and hippocampus. *Mol. Brain* 11:4.
- Giaume, C., Koulakoff, A., Roux, L., Holcman, D., and Rouach, N. (2010). Astroglial networks: a step further in neuroglial and gliovascular interactions. *Nat. Rev. Neurosci.* 11, 87–99. doi: 10.1038/nrn2757
- Giaume, C., Saez, J. C., Song, W., Leybaert, L., and Naus, C. C. (2019). Connexins and pannexins in Alzheimer's disease. *Neurosci. Lett.* 695, 100–105. doi: 10.1016/j.neulet.2017.09.006
- Giaume, C., and Theis, M. (2010). Pharmacological and genetic approaches to study connexin-mediated channels in glial cells of the central nervous system. *Brain Res. Rev.* 63, 160–176. doi: 10.1016/j.brainresrev.2009.11.005
- Giaume, C., and Venance, L. (1998). Intercellular calcium signaling and gap junctional communication in astrocytes. *Glia* 24, 50–64. doi: 10.1002/(sici)1098-1136(199809)24:1<50::aid-glia6>3.0.co;2-4

- Giaume, C. B., Naus, C. C., Saez, J. C., and Leybaert, L. (2020). Glial connexins and pannexins in the healthy and diseased brain. *Physiol. Rev.* 101, 93–145. doi: 10.1152/physrev.00043.2018
- Goldberg, G. S., Lampe, P. D., and Nicholson, B. J. (1999). Selective transfer of endogenous metabolites through gap junctions composed of different connexins. *Nat. Cell Biol.* 1, 457–459. doi: 10.1038/15693
- Goldberg, G. S., Moreno, A. P., and Lampe, P. D. (2002). Gap junctions between cells expressing connexin 43 or 32 show inverse permselectivity to adenosine and ATP. *J. Biol. Chem.* 277, 36725–36730. doi: 10.1074/jbc.M109797200
- Goodenough, D. A., and Paul, D. L. (2009). Gap junctions. *Cold Spring Harb. Perspect. Biol.* 1:a002576.
- Griemann, S., Hoft, S. P., Bedner, P., Zhang, J., Von Staden, E., Beinhauer, A., et al. (2015). Characterization of panglial gap junction networks in the thalamus, neocortex, and hippocampus reveals a unique population of glial cells. *Cereb. Cortex* 25, 3420–3433. doi: 10.1093/cercor/bhu157
- Gutierrez, Y., Garcia-Marques, J., Liu, X., Fortes-Marco, L., Sanchez-Gonzalez, R., Giaume, C., et al. (2019). Sibling astrocytes share preferential coupling via gap junctions. *Glia* 67, 1852–1858. doi: 10.1002/glia.23662
- Han, X., Chen, M., Wang, F., Windrem, M., Wang, S., Shanz, S., et al. (2013). Forebrain engraftment by human glial progenitor cells enhances synaptic plasticity and learning in adult mice. *Cell Stem Cell* 12, 342–353. doi: 10.1016/j.stem.2012.12.015
- Harris, A. L. (2007). Connexin channel permeability to cytoplasmic molecules. *Prog. Biophys. Mol. Biol.* 94, 120–143. doi: 10.1016/j.pbiomolbio.2007.03.011
- Heintz, N. (2004). Gene expression nervous system atlas (GENSAT). *Nat. Neurosci.* 7:483. doi: 10.1038/nn0504-483
- Hille, B. (2001). *Ion Channels of Excitable Cells*. Sunderland, MA: Sinauer.
- Hirtz, J. J., Braun, N., Griesemer, D., Hannes, C., Janz, K., Lohrke, S., et al. (2012). Synaptic refinement of an inhibitory topographic map in the auditory brainstem requires functional Cav1.3 calcium channels. *J. Neurosci.* 32, 14602–14616. doi: 10.1523/jneurosci.0765-12.2012
- Horikawa, K., and Armstrong, W. E. (1988). A versatile means of intracellular labeling: injection of biocytin and its detection with avidin conjugates. *J. Neurosci. Methods* 25, 1–11. doi: 10.1016/0165-0270(88)90114-8
- Houades, V., Koulakoff, A., Ezan, P., Seif, I., and Giaume, C. (2008). Gap junction-mediated astrocytic networks in the mouse barrel cortex. *J. Neurosci.* 28, 5207–5217. doi: 10.1523/jneurosci.5100-07.2008
- Houades, V., Rouach, N., Ezan, P., Kirchhoff, F., Koulakoff, A., and Giaume, C. (2006). Shapes of astrocyte networks in the juvenile brain. *Neuron Glia Biol.* 2, 3–14. doi: 10.1017/s1740925x06000081
- Huang, M., Du, Y., Kiyoshi, C., Wu, X., Askwith, C., Mctigue, D., et al. (2018). Syncytial isopotentiality: an electrical feature of spinal cord astrocyte networks. *Neuroglia* 1, 271–279. doi: 10.3390/neuroglia1010018
- Huang, Q., Zhou, D., and Difiglia, M. (1992). Neurobiotin, a useful neuroanatomical tracer for in vivo anterograde, retrograde and transneuronal tract-tracing and in vitro labeling of neurons. *J. Neurosci. Methods* 41, 31–43. doi: 10.1016/0165-0270(92)90121-s
- Kafitz, K. W., Meier, S. D., Stephan, J., and Rose, C. R. (2008). Developmental profile and properties of sulforhodamine 101-labeled glial cells in acute brain slices of rat hippocampus. *J. Neurosci. Methods* 169, 84–92. doi: 10.1016/j.jneumeth.2007.11.022
- Kang, B. E., Lee, S., and Baker, B. J. (2019). Optical consequences of a genetically-encoded voltage indicator with a pH sensitive fluorescent protein. *Neurosci. Res.* 146, 13–21. doi: 10.1016/j.neures.2018.10.006
- Karram, K., Goebbels, S., Schwab, M., Jennissen, K., Seifert, G., Steinhauser, C., et al. (2008). NG2-expressing cells in the nervous system revealed by the NG2-EYFP-knockin mouse. *Genesis* 46, 743–757. doi: 10.1002/dvg.20440
- Kawata, M., Sano, Y., Inenaga, K., and Yamashita, H. (1983). Immunohistochemical identification of lucifer yellow-labeled neurons in the rat supraoptic nucleus. *Histochemistry* 78, 21–26. doi: 10.1007/bf00491107
- Kettenmann, H., and Ransom, B. R. (1988). Electrical coupling between astrocytes and between oligodendrocytes studied in mammalian cell cultures. *Glia* 1, 64–73. doi: 10.1002/glia.440010108
- Kita, Y., Kawakami, K., Takahashi, Y., and Murakami, F. (2013). Development of cerebellar neurons and glia revealed by in utero electroporation: golgi-like labeling of cerebellar neurons and glia. *PLoS One* 8:e70091. doi: 10.1371/journal.pone.0070091
- Kiyoshi, C. M., Aten, S., Arzola, E. P., Patterson, J. A., Taylor, A. T., Du, Y., et al. (2020). Ultrastructural view of astrocyte-astrocyte and astrocyte-synapse contacts within the hippocampus. *BioRxiv* doi: 10.1101/2020.10.28.358200
- Kiyoshi, C. M., Du, Y., Zhong, S., Wang, W., Taylor, A. T., Xiong, B., et al. (2018). Syncytial isopotentiality: a system-wide electrical feature of astrocytic networks in the brain. *Glia* 66, 2756–2769. doi: 10.1002/glia.23525
- Konietzko, U., and Muller, C. M. (1994). Astrocytic dye coupling in rat hippocampus: topography, developmental onset, and modulation by protein kinase C. *Hippocampus* 4, 297–306. doi: 10.1002/hipo.450040313
- Kuffler, S. W., Nicholls, J. G., and Orkand, R. K. (1966). Physiological properties of glial cells in the central nervous system of amphibia. *J. Neurophysiol.* 29, 768–787. doi: 10.1152/jn.1966.29.4.768
- Kunzelmann, P., Schroder, W., Traub, O., Steinhauser, C., Dermietzel, R., and Willecke, K. (1999). Late onset and increasing expression of the gap junction protein connexin30 in adult murine brain and long-term cultured astrocytes. *Glia* 25, 111–119. doi: 10.1002/(sici)1098-1136(19990115)25:2<111::aid-glia2>3.0.co;2-i
- Langer, J., Stephan, J., Theis, M., and Rose, C. R. (2012). Gap junctions mediate intercellular spread of sodium between hippocampal astrocytes in situ. *Glia* 60, 239–252. doi: 10.1002/glia.21259
- Lee, C. Y., Dallerac, G., Ezan, P., Anderova, M., and Rouach, N. (2016). Glucose tightly controls morphological and functional properties of astrocytes. *Front. Aging Neurosci.* 8:82. doi: 10.3389/fnagi.2016.00082
- Livnah, O., Bayer, E. A., Wilchek, M., and Sussman, J. L. (1993). Three-dimensional structures of avidin and the avidin-biotin complex. *Proc. Natl. Acad. Sci. U.S.A.* 90, 5076–5080. doi: 10.1073/pnas.90.11.5076
- Lunde, L. K., Camassa, L. M., Hoddevik, E. H., Khan, F. H., Ottersen, O. P., Boldt, H. B., et al. (2015). Postnatal development of the molecular complex underlying astrocyte polarization. *Brain Struct. Funct.* 220, 2087–2101. doi: 10.1007/s00429-014-0775-z
- Ma, B., Buckalew, R., Du, Y., Kiyoshi, C. M., Alford, C. C., Wang, W., et al. (2016). Gap junction coupling confers isopotentiality on astrocyte syncytium. *Glia* 64, 214–226. doi: 10.1002/glia.22924
- MacAulay, N. (2020). Molecular mechanisms of K(+) clearance and extracellular space shrinkage-Glia cells as the stars. *Glia* 68, 2192–2211.
- Maglione, M., Tress, O., Haas, B., Karram, K., Trotter, J., Willecke, K., et al. (2010). Oligodendrocytes in mouse corpus callosum are coupled via gap junction channels formed by connexin47 and connexin32. *Glia* 58, 1104–1117. doi: 10.1002/glia.20991
- Matthias, K., Kirchhoff, F., Seifert, G., Huttmann, K., Matyash, M., Kettenmann, H., et al. (2003). Segregated expression of AMPA-type glutamate receptors and glutamate transporters defines distinct astrocyte populations in the mouse hippocampus. *J. Neurosci.* 23, 1750–1758. doi: 10.1523/jneurosci.23-05-01750.2003
- McCutcheon, S., Stout, R. F. Jr., and Spray, D. C. (2020). The dynamic Nexus: gap junctions control protein localization and mobility in distinct and surprising ways. *Sci. Rep.* 10:17011.
- Meier, S. D., Kovalchuk, Y., and Rose, C. R. (2006). Properties of the new fluorescent Na+ indicator CoroNa Green: comparison with SBFI and confocal Na+ imaging. *J. Neurosci. Methods* 155, 251–259. doi: 10.1016/j.jneumeth.2006.01.009
- Meme, W., Vandecasteele, M., Giaume, C., and Venance, L. (2009). Electrical coupling between hippocampal astrocytes in rat brain slices. *Neurosci. Res.* 63, 236–243. doi: 10.1016/j.neures.2008.12.008
- Minta, A., and Tsien, R. Y. (1989). Fluorescent indicators for cytosolic sodium. *J. Biol. Chem.* 264, 19449–19457. doi: 10.1016/s0021-9258(19)47321-3
- Moroni, R. F., Inverardi, F., Regondi, M. C., Pennacchio, P., and Frassoni, C. (2015). Developmental expression of Kir4.1 in astrocytes and oligodendrocytes of rat somatosensory cortex and hippocampus. *Int. J. Dev. Neurosci.* 47, 198–205. doi: 10.1016/j.ijdevneu.2015.09.004
- Moshrefi-Ravaszani, B., Hammel, E. L., Kafitz, K. W., and Rose, C. R. (2017). Astrocyte sodium signalling and panglial spread of sodium signals in brain white matter. *Neurochem. Res.* 42, 2505–2518. doi: 10.1007/s11064-017-2197-9
- Muller, C. M. (1996). “Gap-junctional communication in mammalian cortical astrocytes: development, modifiability and possible functions,” in *Gap Junctions in the Nervous System*, eds D. C. Spray and R. Dermietzel (Austin, TX: RG Landes Company), 203–212. doi: 10.1007/978-3-662-21935-5_12

- Muller, J., Reyes-Haro, D., Pivneva, T., Nolte, C., Schaette, R., Lubke, J., et al. (2009). The principal neurons of the medial nucleus of the trapezoid body and NG2(+) glial cells receive coordinated excitatory synaptic input. *J. Gen. Physiol.* 134, 115–127. doi: 10.1085/jgp.200910194
- Muller, N. I. C., Sonntag, M., Maraslioglu, A., Hirtz, J. J., and Friauf, E. (2019). Topographic map refinement and synaptic strengthening of a sound localization circuit require spontaneous peripheral activity. *J. Physiol.* 597, 5469–5493. doi: 10.1113/jp277757
- Muller, T., Moller, T., Neuhaus, J., and Kettenmann, H. (1996). Electrical coupling among Bergmann glial cells and its modulation by glutamate receptor activation. *Glia* 17, 274–284. doi: 10.1002/(sici)1098-1136(199608)17:4<274::aid-glia2>3.0.co;2-#
- Murphy, A. D., Hadley, R. D., and Kater, S. B. (1983). Axotomy-induced parallel increases in electrical and dye coupling between identified neurons of *Helisoma*. *J. Neurosci.* 3, 1422–1429. doi: 10.1523/jneurosci.03-07-01422.1983
- Nagy, J. I., Patel, D., Ochalski, P. A., and Stelmack, G. L. (1999). Connexin30 in rodent, cat and human brain: selective expression in gray matter astrocytes, co-localization with connexin43 at gap junctions and late developmental appearance. *Neuroscience* 88, 447–468. doi: 10.1016/s0306-4522(98)00191-2
- Nagy, J. I., and Rash, J. E. (2000). Connexins and gap junctions of astrocytes and oligodendrocytes in the CNS. *Brain Res. Brain Res. Rev.* 32, 29–44. doi: 10.1016/s0165-0173(99)00066-1
- Nakase, T., Yoshida, Y., and Nagata, K. (2006). Enhanced connexin 43 immunoreactivity in perinatal areas in the human brain following ischemia. *Glia* 54, 369–375. doi: 10.1002/glia.20399
- Nielsen, M. S., Axelsen, L. N., Sorgen, P. L., Verma, V., Delmar, M., and Holstein-Rathlou, N. H. (2012). Gap junctions. *Compr. Physiol.* 2, 1981–2035.
- Niessen, H., Harz, H., Bedner, P., Kramer, K., and Willecke, K. (2000). Selective permeability of different connexin channels to the second messenger inositol 1,4,5-trisphosphate. *J. Cell Sci.* 113(Pt 8), 1365–1372.
- Nimmerjahn, A., Kirchhoff, F., Kerr, J. N., and Helmchen, F. (2004). Sulforhodamine 101 as a specific marker of astroglia in the neocortex in vivo. *Nat. Methods* 1, 31–37. doi: 10.1038/nmeth706
- Nolte, C., Matyash, M., Pivneva, T., Schipke, C. G., Ohlemeyer, C., Hanisch, U. K., et al. (2001). GFAP promoter-controlled EGFP-expressing transgenic mice: a tool to visualize astrocytes and astroglia in living brain tissue. *Glia* 33, 72–86. doi: 10.1002/1098-1136(20010101)33:1<72::aid-glia1007>3.0.co;2-a
- Nwaobi, S. E., Lin, E., Peramsetty, S. R., and Olsen, M. L. (2014). DNA methylation functions as a critical regulator of Kir4.1 expression during CNS development. *Glia* 62, 411–427. doi: 10.1002/glia.22613
- Olsen, M. L., Khakh, B. S., Skatchkov, S. N., Zhou, M., Lee, C. J., and Rouach, N. (2015). New insights on astrocyte ion channels: critical for homeostasis and neuron-glia signaling. *J. Neurosci.* 35, 13827–13835. doi: 10.1523/jneurosci.2603-15.2015
- Pannasch, U., Vargova, L., Reingruber, J., Ezan, P., Holcman, D., Giaume, C., et al. (2011). Astroglial networks scale synaptic activity and plasticity. *Proc. Natl. Acad. Sci. U.S.A.* 108, 8467–8472. doi: 10.1073/pnas.1016650108
- Rackauskas, M., Verselis, V. K., and Bukauskas, F. F. (2007). Permeability of homotypic and heterotypic gap junction channels formed of cardiac connexins mCx30.2, Cx40, Cx43, and Cx45. *Am. J. Physiol. Heart Circ. Physiol.* 293, H1729–H1736.
- Ransom, B. R., and Goldring, S. (1973). Ionic determinants of membrane potential of cells presumed to be glia in cerebral cortex of cat. *J. Neurophysiol.* 36, 855–868. doi: 10.1152/jn.1973.36.5.855
- Ransom, B. R., and Kettenmann, H. (1990). Electrical coupling, without dye coupling, between mammalian astrocytes and oligodendrocytes in cell culture. *Glia* 3, 258–266. doi: 10.1002/glia.440030405
- Rouach, N., Koulakoff, A., Abudara, V., Willecke, K., and Giaume, C. (2008). Astroglial metabolic networks sustain hippocampal synaptic transmission. *Science* 322, 1551–1555. doi: 10.1126/science.1164022
- Scemes, E., and Giaume, C. (2006). Astrocyte calcium waves: what they are and what they do. *Glia* 54, 716–725. doi: 10.1002/glia.20374
- Schools, G. P., Zhou, M., and Kimelberg, H. K. (2006). Development of gap junctions in hippocampal astrocytes: evidence that whole cell electrophysiological phenotype is an intrinsic property of the individual cell. *J. Neurophysiol.* 96, 1383–1392. doi: 10.1152/jn.00449.2006
- Schreiner, A. E., Durry, S., Aida, T., Stock, M. C., Ruther, U., Tanaka, K., et al. (2014). Laminar and subcellular heterogeneity of GLAST and GLT-1 immunoreactivity in the developing postnatal mouse hippocampus. *J. Comp. Neurol.* 522, 204–224. doi: 10.1002/cne.23450
- Seifert, G., Huttmann, K., Binder, D. K., Hartmann, C., Wyczynski, A., Neusch, C., et al. (2009). Analysis of astroglial K⁺ channel expression in the developing hippocampus reveals a predominant role of the Kir4.1 subunit. *J. Neurosci.* 29, 7474–7488. doi: 10.1523/jneurosci.3790-08.2009
- Sontheimer, H., Waxman, S. G., and Ransom, B. R. (1991). Relationship between Na⁺ current expression and cell-cell coupling in astrocytes cultured from rat hippocampus. *J. Neurophysiol.* 65, 989–1002. doi: 10.1152/jn.1991.65.4.989
- Speizer, L., Haugland, R., and Kutchai, H. (1985). Asymmetric transport of a fluorescent glucose analogue by human erythrocytes. *Biochim. Biophys. Acta* 815, 75–84. doi: 10.1016/0005-2736(85)90476-6
- Stephan, J., and Friauf, E. (2014). Functional analysis of the inhibitory neurotransmitter transporters GlyT1, GAT-1, and GAT-3 in astrocytes of the lateral superior olive. *Glia* 62, 1992–2003. doi: 10.1002/glia.22720
- Stephan, J., Haack, N., Kafitz, K. W., Durry, S., Koch, D., Hochstrate, P., et al. (2012). Kir4.1 channels mediate a depolarization of hippocampal astrocytes under hyperammonemic conditions in situ. *Glia* 60, 965–978. doi: 10.1002/glia.22328
- Susaki, E. A., Tainaka, K., Perrin, D., Kishino, F., Tawara, T., Watanabe, T. M., et al. (2014). Whole-brain imaging with single-cell resolution using chemical cocktails and computational analysis. *Cell* 157, 726–739. doi: 10.1016/j.cell.2014.03.042
- Susaki, E. A., Tainaka, K., Perrin, D., Yukinaga, H., Kuno, A., and Ueda, H. R. (2015). Advanced CUBIC protocols for whole-brain and whole-body clearing and imaging. *Nat. Protoc.* 10, 1709–1727. doi: 10.1038/nprot.2015.085
- Tasker, J. G., Hoffman, N. W., and Dudek, F. E. (1991). Comparison of three intracellular markers for combined electrophysiological, morphological and immunohistochemical analyses. *J. Neurosci. Methods* 38, 129–143. doi: 10.1016/0165-0270(91)90163-t
- Terman, D., and Zhou, M. (2019). Modeling the role of the astrocyte syncytium and K⁺ buffering in maintaining neuronal firing patterns. *Opera Med. Physiol.* 5, 7–16.
- Veenstra, R. D. (1996). Size and selectivity of gap junction channels formed from different connexins. *J. Bioenerg. Biomembr.* 28, 327–337. doi: 10.1007/bf02110109
- Veenstra, R. D., Wang, H. Z., Beblo, D. A., Chilton, M. G., Harris, A. L., Beyer, E. C., et al. (1995). Selectivity of connexin-specific gap junctions does not correlate with channel conductance. *Circ. Res.* 77, 1156–1165. doi: 10.1161/01.res.77.6.1156
- Wadle, S. L., Augustin, V., Langer, J., Jabs, R., Philippot, C., Weingarten, D. J., et al. (2018). Anisotropic panglial coupling reflects tonotopic organization in the inferior colliculus. *Front. Cell Neurosci.* 12:431. doi: 10.3389/fncel.2018.00431
- Wallraff, A., Kohling, R., Heinemann, U., Theis, M., Willecke, K., and Steinhauser, C. (2006). The impact of astrocytic gap junctional coupling on potassium buffering in the hippocampus. *J. Neurosci.* 26, 5438–5447. doi: 10.1523/jneurosci.0037-06.2006
- Wallraff, A., Odermatt, B., Willecke, K., and Steinhauser, C. (2004). Distinct types of astroglial cells in the hippocampus differ in gap junction coupling. *Glia* 48, 36–43. doi: 10.1002/glia.20040
- Wang, H. Z., and Veenstra, R. D. (1997). Monovalent ion selectivity sequences of the rat connexin43 gap junction channel. *J. Gen. Physiol.* 109, 491–507. doi: 10.1085/jgp.109.4.491
- Wang, Q., Wang, W., Aten, S., Kiyoshi, C. M., Du, Y., and Zhou, M. (2020). Epileptiform neuronal discharges impair astrocyte syncytial isopotentiality in acute hippocampal slices. *Brain Sci.* 10:208. doi: 10.3390/brainsci10040208
- Wang, W., Kiyoshi, C. M., Du, Y., Taylor, A. T., Sheehan, E. R., Wu, X., et al. (2020). TREK-1 null impairs neuronal excitability, synaptic plasticity, and cognitive function. *Mol. Neurobiol.* 57, 1332–1346. doi: 10.1007/s12035-019-01828-x
- Wasseff, S. K., and Scherer, S. S. (2011). Cx32 and Cx47 mediate oligodendrocyte-astrocyte and oligodendrocyte-oligodendrocyte gap junction coupling. *Neurobiol. Dis.* 42, 506–513. doi: 10.1016/j.nbd.2011.03.003
- Weber, P. A., Chang, H. C., Spaeth, K. E., Nitsche, J. M., and Nicholson, B. J. (2004). The permeability of gap junction channels to probes of different size is dependent on connexin composition and permeant-pore affinities. *Biophys. J.* 87, 958–973. doi: 10.1529/biophysj.103.036350
- Wu, L., Dong, A., Dong, L., Wang, S. Q., and Li, Y. (2019). PARIS, an optogenetic method for functionally mapping gap junctions. *eLife* 8:e43366.

- Xin, W., Schuebel, K. E., Jair, K. W., Cimbro, R., De Biase, L. M., Goldman, D., et al. (2019). Ventral midbrain astrocytes display unique physiological features and sensitivity to dopamine D2 receptor signaling. *Neuropsychopharmacology* 44, 344–355. doi: 10.1038/s41386-018-0151-4
- Xu, G., Wang, W., Kimelberg, H. K., and Zhou, M. (2010). Electrical coupling of astrocytes in rat hippocampal slices under physiological and simulated ischemic conditions. *Glia* 58, 481–493.
- Xu, G., Wang, W., and Zhou, M. (2014). Spatial organization of NG2 glial cells and astrocytes in rat hippocampal CA1 region. *Hippocampus* 24, 383–395. doi: 10.1002/hipo.22232
- Yagi, T., Terada, N., Baba, T., and Ohno, S. (2002). Localization of endogenous biotin-containing proteins in mouse Bergmann glial cells. *Histochem. J.* 34, 567–572.
- Yamada, K., Nakata, M., Horimoto, N., Saito, M., Matsuoka, H., and Inagaki, N. (2000). Measurement of glucose uptake and intracellular calcium concentration in single, living pancreatic beta-cells. *J. Biol. Chem.* 275, 22278–22283. doi: 10.1074/jbc.m908048199
- Yang, Y., Vidensky, S., Jin, L., Jie, C., Lorenzini, I., Frankl, M., et al. (2011). Molecular comparison of GLT1+ and ALDH1L1+ astrocytes in vivo in astroglial reporter mice. *Glia* 59, 200–207. doi: 10.1002/glia.21089
- Yoshioka, K., Saito, M., Oh, K. B., Nemoto, Y., Matsuoka, H., Natsume, M., et al. (1996). Intracellular fate of 2-NBDG, a fluorescent probe for glucose uptake activity, in *Escherichia coli* cells. *Biosci. Biotechnol. Biochem.* 60, 1899–1901. doi: 10.1271/bbb.60.1899
- Zhong, S., Du, Y., Kiyoshi, C. M., Ma, B., Alford, C. C., Wang, Q., et al. (2016). Electrophysiological behavior of neonatal astrocytes in hippocampal stratum radiatum. *Mol. Brain* 9:34.
- Zhou, M., Schools, G. P., and Kimelberg, H. K. (2006). Development of GLAST(+) astrocytes and NG2(+) glia in rat hippocampus CA1: mature astrocytes are electrophysiologically passive. *J. Neurophysiol.* 95, 134–143. doi: 10.1152/jn.00570.2005

Conflict of Interest: The authors declare that the research was conducted in the absence of any commercial or financial relationships that could be construed as a potential conflict of interest.

Copyright © 2021 Stephan, Eitelmann and Zhou. This is an open-access article distributed under the terms of the Creative Commons Attribution License (CC BY). The use, distribution or reproduction in other forums is permitted, provided the original author(s) and the copyright owner(s) are credited and that the original publication in this journal is cited, in accordance with accepted academic practice. No use, distribution or reproduction is permitted which does not comply with these terms.